Morari Michele (Orcid ID: 0000-0002-4601-4454)

RGS4 negatively modulates Nociceptin/Orphanin FQ opioid receptor signaling: implication for L-Dopa-induced dyskinesia.

Running title: RGS4 negatively modulates NOP receptor

[1]Pisanò CA, [1]Mercatelli D, [2]Mazzocchi M, [1]Brugnoli A, [3]Morella I, [3]Fasano S, [4]Zaveri NT, [3,5]Brambilla R, [2]O'Keeffe GW, [6]Neubig RR, [1]Morari M.

[1]Department of Neuroscience and Rehabilitation, Section of Pharmacology, University of Ferrara, via Fossato di Mortara 17-19, 44121 Ferrara, Italy.

[2]Department of Anatomy and Neuroscience, University College Cork, Cork, Ireland.

[3]Neuroscience and Mental Health Research Institute, Division of Neuroscience, School of Biosciences, Cardiff University, CF24 4HQ, Cardiff, UK.

[4]Astraea Therapeutics, 320 Logue Avenue, Suite 142, Mountain View, CA 94043, USA

[5]Department of Biology and Biotechnology "L. Spallanzani", University of Pavia, Via Ferrata 9, 27100 Pavia, Italy

[6]Dept. Pharmacology and Toxicology, Michigan State University, East Lansing, MI 48824, USA

Word count: 3707

Acknowledgements

This study was funded by local grants from the University of Ferrara (#FAR1891100). We thank Dr Susanne M Mumby for generous gift of the RGS4 antibody, and Jeffrey Leipprandt and Behirda Karaj for technical assistance.

Conflict of interest statement

The authors declare no conflict of interest

Data availability

The data that support the findings of this study are available from the corresponding author upon reasonable request. Some data may not be made available because of privacy or ethical restrictions

Corresponding author: Michele Morari, PhD, Department of Neuroscience and Rehabilitation, Section of Pharmacology, University of Ferrara, via Fossato di Mortara 17-19, 44121 Ferrara (Italy), email: m.morari@unife.it.

ORCID ID: Michele Morari 0000-0002-4601-4454

Bullet point summary

What is already known

- RGS4 is a signal transduction protein that inactivates signaling at $G\alpha_{i/o}$ and $G\alpha_{q}$-coupled GPCRs.
- RGS4 reduces signaling by μ and δ opioid receptors.

What this study adds

- RGS4 inhibits nociceptin/orphanin FQ opioid (NOP) receptor-mediated responses in vitro while RGS4 blockade potentiates them.
- RGS4 blockade potentiates NOP agonist-mediated attenuation of levodopa-induced dyskinesia and its neurochemical correlates.

Clinical significance

- RGS4 inhibitors could potentiate antidyskinetic activity of NOP receptor agonists and widen their safety window.

Author contributions

Clarissa Anna Pisanò and Michele Morari conceived the study, designed the experiments, and drafted the final version of the manuscript. Gerard W. O'Keeffe, Richard R. Neubig, Riccardo Brambilla designed and supervised the experiments in *ìn vitro* models. Clarissa Anna Pisanò performed experiments in cell lines and dyskinetic rats. Martina Mazzocchi performed experiments in primary striatal neurons. Daniela Mercatelli performed Western blot analysis. Alberto Brugnoli performed behavioural experiments in $RGS4^{-/-}$ mice. Ilaria

Morella and Stefania Fasano performed experiments in mouse slices. Nurulain T Zaveri critically revised NOP pharmacology and synthesised AT-403. All authors reviewed and edited the manuscript.

Non standard abbreviations

AIMs, abnormal involuntary movements; ALO, axial, limb and orolingual; DA, dopamine; δ, delta opioid peptide; DARPP-32, dopamine and cAMP-regulated phosphoprotein 32 kDa; ERK, extracellular signal regulated kinase 1 and 2; κ, kappa opioid peptide; L-Dopa, levodopa; LID, levodopa-induced dyskinesia; μ, mu opioid peptide; MSNs, medium-sized spiny neurons; N/OFQ, nociceptin/orphanin FQ; NOP, nociceptin/orphanin FQ opioid peptide; 6-OHDA, 6-hydroxydopamine; PD, Parkinson's disease; RGS4, Regulator of G-protein signal 4; SNr, substantia nigra reticulata.

Abstract

Background and purpose: Regulator of G-protein signal 4 (RGS4) is a signal transduction protein that accelerates intrinsic GTPase activity of $G\alpha_{i/o}$ and $G\alpha_q$ subunits, suppressing GPCR signaling. Here we investigate whether RGS4 modulates nociceptin/orphanin FQ (N/OFQ) opioid (NOP) receptor signaling and this modulation has relevance for L-Dopa-induced dyskinesia.

Experimental approach: HEK293T cells transfected with NOP, NOP/RGS4 or NOP/RGS19 were challenged with N/OFQ and the small molecule NOP agonist AT-403, using D1-stimulated cAMP levels as a readout. Primary rat striatal neurons and adult mouse striatal slices were challenged with N/OFQ or AT-403 in the presence of the experimental RGS4 chemical probe, CCG-203920, and D1-stimulated cAMP or phosphorylated extracellular signal regulated kinase 1/ 2 (pERK) responses were monitored. In vivo, CCG-203920 was co-administered with AT-403 and L-Dopa to 6-hydroxydopamine hemilesioned

rats, and dyskinetic movements, striatal biochemical correlates of dyskinesia (pERK and pGluR1 levels) and striatal RGS4 levels were measured.

Key results: RGS4 expression reduced NOFQ and AT-403 potency and efficacy in HEK293T cells. CCG-203920 increased N/OFQ potency in primary rat striatal neurons, and potentiated AT-403 response in mouse striatal slices. CCG-203920 enhanced AT-403 mediated inhibition of dyskinesia and its biochemical correlates, without compromising its motor-improving effects. Unilateral dopamine depletion caused bilateral reduction of RGS4 levels, which was reversed by L-Dopa. L-Dopa acutely upregulated RGS4 in the lesioned striatum.

Conclusions and Implications: RGS4 physiologically inhibits NOP receptor signaling. CCG-203920 enhanced NOP responses and improved the antidyskinetic potential of NOP receptor agonists, mitigating the effects of striatal RGS4 upregulation occurring during dyskinesia expression.

Keywords: AT-403, CCG-203920, dyskinesia, L-Dopa, nociceptin/orphanin FQ, RGS4.

1. Introduction

Regulators of G protein signaling (RGS) are signal transduction proteins which couple to heterotrimeric G protein coupled receptors (GPCRs). RGS proteins bind to the Gα-GTP complex and accelerate its intrinsic GTPase activity, promoting the formation of Gα-GDP and the reassembly of Gαβγ trimer. This causes the termination of GPCR-driven intracellular signaling (Berman *et al.*, 1996; Tesmer *et al.*, 1997). RGS proteins are grouped into five subfamilies (R4, R7, R12, RA and RZ) based on sequence homology. They interact with $G\alpha_i$, $G\alpha_o$, $G\alpha_{12/13}$ but not $G\alpha_s$, and show a variable degree of receptor and G-protein specificity (Kimple *et al.*, 2011; Sjogren, 2017). Different subtypes of RGS have been shown to modulate opioid receptors (Traynor, 2012), and have been proposed as a novel therapeutic

targets for pain, depression and addiction (Gross *et al.*, 2019; Sakloth *et al.*, 2020; Senese *et al.*, 2020; Stratinaki *et al.*, 2013; Traynor *et al.*, 2005). In particular, RGS type 4 (RGS4) has been shown to regulate μ opioid (Xie *et al.*, 2005) and δ opioid (Dripps *et al.*, 2017) receptors, RGS type 9 isoform 2 (RGS9-2) regulates μ opioid receptors (Garzon *et al.*, 2001; Psifogeorgou *et al.*, 2007; Zachariou *et al.*, 2003) and RGS type 12 (RGS12) regulates κ opioid receptors (Gross *et al.*, 2019). Preliminary in vitro evidence suggests that RGS type 19 (RGS19) modulates the NOP receptor (Xie *et al.*, 2005). The NOP receptor is a "non-opioid" member of the opioid receptor family, endogenously activated by its natural heptadecapeptide ligand Nociceptin/Orphanin FQ (N/OFQ). N/OFQ regulates several central and peripheral functions (Toll *et al.*, 2016) and is involved in motor disorders, such as Parkinson disease (PD) and L-Dopa-induced dyskinesia (LID) (Mercatelli *et al.*, 2020), a major disabling complication of L-Dopa pharmacotherapy of PD (Bastide *et al.*, 2015). Specifically, NOP receptor antagonists proved effective in attenuating motor symptoms and neuropathology associated with experimental parkinsonism whereas NOP receptor agonists proved effective as antidyskinetic agents in animal models of LID (Arcuri *et al.*, 2018; Marti *et al.*, 2012). However, small molecule NOP receptor agonists also produced strong hypolocomotion/sedation, which partly masked their antidyskinetic effects (Arcuri *et al.*, 2018). Therefore, in view of the fact that RGS can modulate specific behavioral outcomes of δ opioid and μ opioid receptor stimulation (Jutkiewicz *et al.*, 2005), we hypothesized that targeting RGS4 would improve the antidyskinetic effects of NOP receptor agonists relative to their hypolocomotive/sedative effects which would widen their safety window. In the present study, we investigated the interaction of NOP with a specific subtype of RGS, namely RGS4, and its relevance for LID in vivo. RGS4 and NOP receptor are expressed in brain areas relevant to LID, such as cortex, striatum and substantia nigra (Ebert *et al.*, 2006; Gold *et al.*, 1997; Neal *et al.*, 1999). Moreover, both RGS4 and NOP are expressed by medium-sized

GABAergic striatal neurons, which are the main neurobiological substrate of LID (Ebert *et al.*, 2006; Neal *et al.*, 1999). RGS4 is involved in LID development and expression, and blockade of RGS4 with an antisense nucleotide improved dyskinesia in a rat model of LID (Ko *et al.*, 2014).

In this study, the functional interaction between RGS4 and NOP receptor was investigated first in a cellular model (HEK293T cells) artificially overexpressing both proteins, then in native tissues, i.e. rat primary striatal cultures and striatal slices of adult mouse. In native tissues, the RGS4 selective experimental RGS4 chemical probe CCG-203920 (Turner *et al.*, 2012) was used to pharmacologically inhibit RGS4 and potentiate NOP receptor responses. The ability of CCG-203920 to potentiate the inhibitory effect of the potent and selective small molecule NOP receptor agonist AT-403 (Arcuri *et al.*, 2018) on LID and its biochemical correlates (i.e. pERK and pGluR1 upregulation) was then tested in vivo. The levels of RGS4 protein in the dyskinetic striatum, both OFF and ON L-Dopa were also measured.

2. Methods

Studies were designed to generate groups of equal size, using randomization and blinded analysis to comply with BJP guidelines (Curtis *et al.*, 2018). Experimental protocols were conducted according to the Directive 2010/63/EU and in compliance with the ARRIVE guidelines (Percie du Sert *et al.*, 2020) and BJP recommendations (Lilley *et al.*, 2020).

2.1 Animal subjects

One hundred ten (110) male Sprague-Dawley rats (150 g; Charles River Lab, Calco, Lecco, Italy; RGD Cat# 734476, RRID:RGD_734476) were used in this study. Seven (7) naïve rats were kept for WB analysis of RGS4 levels (Fig. 7) whereas 103 underwent 6-OHDA lesioning. Eighty-five (85) 6-OHDA rats passed the selection criteria (see below): 7 were

used for WB studies (Figs. 5-7) and 78 underwent chronic treatment with L-Dopa. At the end of L-Dopa treatment, we obtained 59 dyskinetic rats (ALO AIM score ≥100), of which 35 were kept for WB studies and 24 for behavioral analysis. Sixteen (16) RGS4 knockout ($RGS4^{-/-}$, RRID:IMSR_JAX:005833) backcrossed on C57BL/6J and 16 C57BL/6J wild-type male mice (24-26 g, 10-12 weeks old; RRID:IMSR_JAX:000664) were used for the analysis of RGS4 selectivity of CCG-203920 and RGS4 antibody specificity (Fig. S1). Specifically, 10 $RGS4^{-/-}$ mice and 10 C57BL/6J wild-type controls were used for behavioral studies with CCG-203920, and other 6 $RGS4^{-/-}$ mice and 6 C57BL/6J controls were used for Western blot analysis. C57BL/6J $RGS4^{-/-}$ mice, originally developed by Dr S Heximer (University of Toronto) (Cifelli *et al.*, 2008), were provided by Dr RR Neubig and colony raised at the University of Ferrara. Animals were housed in a specific pathogen-free (SPF) standard facility (LARP) of the University of Ferrara with free access to food (4RF21 standard diet; Mucedola, Settimo Milanese, Milan, Italy) and water, and kept under regular lighting conditions (12 hr dark/light cycle). Animals were housed in groups with environmental enrichments. Adequate measures were taken to minimize animal pain and discomfort. Rats were sacrificed with an overdose of isoflurane or with isoflurane anaesthesia followed by decapitation (WB studies), mice with isoflurane anaesthesia followed by cervical dislocation. Experimental protocols were approved by the Ethical Committee of the University of Ferrara and the Italian Ministry of Health (licenses 714/2016-PR and 368/2018). Ten (10) time-mated pregnant female Sprague-Dawley rats were used to generate primary cultures of the striatum. There were housed in the Biological Service Unit, at University College Cork under regular conditions of lights (12h light/dark cycle) with *ad libitum* access to food and water. On embryonic day (E) 14, embryos (106 in total) were removed by laparotomy from euthanized dams and used to generated primary cultures of the rat striatum as outlined below (license number AE19130/ I304). Seven 12-week-old male C57BL6 mice were used for ERK studies

in slices in vitro. Mice were housed in a standard facility at Cardiff University, under regular conditions of light (12 h light/dark cycle), with food and water ad libitum.

2.2 In vitro experiments

2.2.1 Cell culture and transfection

Human embryonic kidney cells (HEK293T; ECACC Cat# 12022001, RRID:CVCL_0063) were maintained in a humidified incubator at 37°C with 5% CO2 and grown to 90-95% confluence in Dulbecco's modified Eagle's medium (DMEM) supplemented with 10% fetal bovine serum (FBS), 100 U ml^{-1} penicillin and 100 µg ml^{-1} streptomycin. Cells were transfected with the D1 dopamine receptor (1 ng/well), $G\alpha_s$ (0.1 ng/well), and NOP (1 ng/well) using Lipofectamine 2000 according to the manufacturer's recommended protocol. All transfections were performed under serum-free conditions in Opti-MEM. Transfections were allowed to proceed for 4-5 h before the media was changed back to DMEM with 10 % FBS. Experiments were run 24 h after transfection. For cAMP assays, cells were plated in 6-mm dishes. DNA was kept constant at 6 µg and 6 µl of Lipofectamine2000 per plate was used. Empty vector (pcDNA3.1+, RRID:Addgene_10842) was used to adjust the total amount of DNA. The lack of cAMP stimulation in control vector (pcDNA3.1+) transfected cells and the robust change in cAMP levels in D1/NOP transfected cells after treatment with specific ligands were used to establish the success of transfection (Feng *et al.*, 2017). This is possible because HEK293T cells do not natively express D1 and NOP receptors.

2.2.2 cAMP measurements in HEK293T cells

LANCE Ultra cAMP assays (Perkin Elmer; Waltham, MA) were performed in accordance with the manufacturer's instructions. Briefly, the day before the assay, HEK293T cells were transfected as indicated above. On the day of experiment, cells were dissociated from dishes using Versene 1M. Then cells (2,000 cells/well in 5µl) were transferred to a white 384-well microplate (Perkin Elmer) and incubated with various concentrations of N/OFQ and SKF-

38393 (D1 receptor agonist; final 40 nM; 5 µl/well) for 30 min at room temperature. A cAMP standard curve was generated in triplicate according to the manual. Finally, europium (Eu)-cAMP tracer (5 µl) and ULight™-anti-cAMP (5 µl) were added to each well and incubated for 1 h at room temperature. The plate was read on a TR-FRET microplate reader (Synergy NEO; Biotek, Winooski, VT).

2.2.3 ERK measurement in vitro

Adult male C57BL/6J mice were decapitated after anaesthesia and cervical dislocation, and brain slices were freshly prepared according to the protocol previously described (Arcuri *et al.*, 2018; Marti *et al.*, 2012). The brains were rapidly removed and put on a cool glass plate filled with ice-cold sucrose-based dissecting solution (87 mM NaCl, 2.5 mM KCl, 7 mM MgCl2, 1 mM NaH2PO4, 75 mM sucrose, 25 mM NaHCO3, 10 mM D-glucose, 0.5 mM CaCl2, 2 mM kynurenic acid), carbogenated (95% O2, 5% CO2) and subsequently mounted on the vibratome stage (Vibratome, VT1000S-Leica Microsystems); 200-µm-thick slices were cut and transferred into a brain slice chamber (Brain slice chamber-BSC1, Scientific System design Inc., Mississauga, ON, Canada) and allowed to recover for 1 h at 32°C, with a constant perfusion of carbogenated artificial CSF (ACSF: 124 mM NaCl, 5 mM KCl, 1.3 mM $MgSO_4$, 1.2 mM NaH_2PO_4, 25 mM $NaHCO_3$, 10 mM D-glucose, 2.4 mM $CaCl_2$). The D1 receptor agonist SKF-38393 (100 µM) was applied for 10 min in the presence of AT-403 (30 nM), CCG203920 (500 nM) or vehicle. After fixation in 4% paraformaldehyde (PFA) for 15 min at room temperature, slices were rinsed three times in PBS and cryoprotected in 30% sucrose solution overnight at 4°C. On the following day, slices were further cut into 18-µm-thick slices using a cryostat (Leica CM1850) and mounted onto SuperFrost Plus slides (Thermo Fisher Scientific). Immunohistochemistry was performed as previously described (Papale *et al.*, 2016): 1 h after blocking in 5% normal goat serum and 0.1% Triton X-100 solution, slices were incubated overnight at 4°C with anti-phospho-p44/42 MAP kinase

(Thr202/Tyr204) (Cell Signaling Technology Cat# 4370 RRID:AB_2315112, 1:1000). Sections were then incubated with biotinylated goat anti-rabbit IgG (1:200, Vector Laboratories, Cat# BA 1000 RRID:AB_2313606) for 2 h at room temperature. Detection of the bound antibodies was carried out using a standard peroxidase-based method (Vectastain Elite ABC kit Cat# PK-7100, RRID:AB_2336827, Vector Laboratories), followed by a 3,3'-diamino-benzidine (DAB) and H_2O_2 solution. Images were acquired from the striatum at 40× magnification using a brightfield microscope (Leica Macro/Micro Imaging System), and the number of pERK positive cells in the striatum was counted in each slice.

2.2.4 Primary striatal neuron cultures

Primary cultures of embryonic (E) day 14 rat ganglionic eminence (hereafter referred to as striatum) (from the Biological Service Unit, University College Cork) were dissected as previously described (Schmidt *et al.*, 2012). All scientific procedures were performed under a license in accordance with the European Communities Council Directive (86/609/EEC) and approval by local Animal Experimentation Ethics Committee. After dissection, the tissue was dissociated and neurons were plated in poly-D-lysine coated 24-well plates (Sigma) in DMEM:F12 media (Sigma) supplemented with 1% penicillin/streptomycin (Sigma), 1% L-glutamine (Sigma), 2% B27 (Invitrogen) and 1% FBS. Cells were maintained in culture for 7DIV.

2.2.5 cAMP measurements in primary striatal neurons

On day 8 of culture, where indicated cells were treated for 30 min with SKF-38393 (100 μM), CCG-203920 (100 nM) and/or N/OFQ (0.01-1 nM). Cultures were then fixed for 15 min in 4% paraformaldehyde. Following 3 × 5 min washes in 10 mM PBS-T (0.02% Triton X-100 in 10 mM PBS), cultures were incubated in 5% bovine serum albumin (BSA) in 10 mM PBS-T for 1 h at room temperature. Cultures were subsequently incubated in the following primary antibodies: DARPP32 (R and D Systems Cat# AF6259,

RRID:AB_10641854; 1:500), cAMP (R and D Systems Cat# MAB2146, RRID:AB_495027; 1:500), diluted in 1% BSA in 10 mM PBS at 4°C overnight. Following 3 × 5 min washes in 10 mM PBS-T, cells were incubated in 594-conjugated secondary antibodies (Thermo Fisher Scientific Cat# A-11005, RRID:AB_2534073, 1:500) in 1% BSA prior to 3 × 5 min washes. Cells were imaged using an Olympus IX71 inverted microscope. The fluorescence intensity of individual cells was measured by densitometry using Image J analysis software (ImageJ, RRID:SCR_003070).

2.3 In vivo experiments

2.3.1 Evaluation of RGS4 selectivity of CCG-203920 in mice

As we previously reported (Blazer *et al.*, 2015) that RGS4 inhibitors reverse raclopride-induced akinesia in the bar and drag tests (Marti *et al.*, 2004; Viaro *et al.*, 2008), the same tests were used to monitor motor activity in 5 $RGS4^{-/-}$ mice and 5 wild-type controls treated with 1 mg kg^{-1} (i.p.) raclopride and, 30 min later, by 10 mg kg^{-1} CCG-203920 or saline (i.p.). Prior to pharmacological testing, mice were trained daily for a week on the behavioral tests until their motor performance became reproducible. The bar (or catalepsy) test measures the ability of the animal to respond to an externally imposed static posture. Each mouse was placed gently on a table and the right and left forepaws were placed alternately on blocks of increasing heights (1.5, 3, and 6 cm). Total time spent on the blocks (in seconds) by each paw was recorded (cutoff time 20 s per block, 60 s maximum) and pooled together. The drag test measures the number of steps made by the animal when gently lifted by the tail (allowing the forepaws on the table) and dragged backward at a constant speed (about 20 cm s^{-1}) for a fixed distance (100 cm). The number of steps made by each forepaw was counted by two separate blinded observers and average together.

2.3.2 Experimental design

A cohort of 10 RGS4$^{-/-}$ mice was allotted in two groups (n=5 each) receiving raclopride followed by CCG-203920 or saline. Four days later, treatments were crossed. The same protocol was adopted for 10 wild-type control mice.

2.3.4 Unilateral 6-OHDA lesion

The unilaterally 6-OHDA lesioned rat, the most popular and best validated rodent model of Parkinson's disease and LID (Cenci *et al.*, 2018; Duty *et al.*, 2011; Schwarting *et al.*, 1996) was used. One-hundred three (103) naïve rats (150 g) were unilaterally injected under isoflurane anesthesia in the (right) medial forebrain bundle with 12 µg of 6-OHDA free base (dissolved in 0.02% ascorbate-saline), according to the following stereotaxic coordinates from bregma and the dural surface (in mm): antero-posterior (AP) -4.4, medio-lateral (ML) 1.2, dorso-ventral (DV) -7.8, tooth bar at -2.4 mm (Paxinos *et al.*, 1986), as previously described (Arcuri *et al.*, 2018; Marti *et al.*, 2012; Pisanò *et al.*, 2020). Animals were pretreated with antibiotics (Synulox^{TM}, 50 µl/Kg, i.p.), and the wound was sutured and infiltrated with 2% lidocaine solution (Esteve^{TM}). Two weeks later, rats were screened by assessing the motor asymmetry score in two different ethological tests (the bar and drag tests) (Marti *et al.*, 2005). Rats showing immobility time >20 sec at the contralateral paw in the bar test, and <3 steps at the contralateral paw (or alternatively a contralateral/ipsilateral paw ratio <50%) were used in the study (Brugnoli *et al.*, 2020; Pisanò *et al.*, 2020).

2.3.5 L-Dopa treatment and abnormal involuntary movement rating

Seventy-eight (78) rats that successfully passed the threshold values in the bar and drag test were treated for 21 days with L-Dopa (6 mg kg^{-1} + benserazide 15 mg kg^{-1}, s.c., once daily) to induce abnormal involuntary movements (AIMs), a correlate of LID (Cenci *et al.*, 1998; Cenci *et al.*, 2007), as previously described (Brugnoli *et al.*, 2020; Marti *et al.*, 2012; Paolone *et al.*, 2015). Rats were observed for 1 min, every 20 min, during the 3 h that followed L-DOPA injection or until dyskinetic movements ceased. Dyskinetic movements were

classified based on their topographical distribution into three subtypes: (i) axial AIM, that is, twisted posture or turning of the neck and upper body toward the side contralateral to the lesion; (ii) forelimb AIM, that is, jerky and dystonic movements and/or purposeless grabbing of the forelimb contralateral to the lesion; and (iii) orolingual AIM, that is, orofacial muscle twitching, purposeless masticatory movements and contralateral tongue protrusion. Each AIM subtype was rated on a frequency scale from 0 to 4 (1, occasional; 2, frequent; 3, continuous but interrupted by an external distraction; 4, continuous and not interrupted by an external distraction). In addition, the amplitude of these AIMs was measured on a scale from 0 to 4 based on a previously validated scale (Cenci *et al.*, 2007). Axial, Limb and Orolingual (ALO) AIMs total value were obtained as the sum of the product between amplitude and frequency of each observation (Cenci *et al.*, 2007), and fully dyskinetic rats scored ≥100.

2.3.6 Experimental design

Twelve (12) fully dyskinetic rats were randomized to L-Dopa (6 mg kg^{-1} + benserazide 15 mg kg^{-1}, s.c.) in combination with AT-403 (0.03 mg kg^{-1}), CCG-203920 (10 mg kg^{-1}), AT-403 + CCG-203920, or saline. Each animal was tested four times, with a 3-day washout allowed between treatments. To evaluate whether the potential antidyskinetic effect was associated with an improvement of global motor activity (Arcuri *et al.*, 2018; Marti *et al.*, 2012; Paolone *et al.*, 2015), a separate cohort of 12 rats was subjected to the same treatments as above for the analysis of motor performance on the rotarod, both before (OFF L-Dopa) and after L-Dopa administration (ON L-Dopa), In fact, a truly antidyskinetic compound would alleviate LID and consequently improve rotarod performance whereas a motor inhibiting or a sedative agent would reduce AIMs along with motor performance. Rotarod performance was assessed at 60 min after L-Dopa administration since the ALO AIMs time course showed a peak 60-80 min after L-Dopa administration (Arcuri *et al.*, 2018; Marti *et al.*, 2012; Paolone *et al.*, 2015).

2.3.7 Western blot analysis

Western blotting analysis complies with the recommendations of the British Journal of Pharmacology (Alexander *et al.*, 2018). Thirty-five (35) dyskinetic rats were saved for this experiment, but one rat was sacrificed for reaching humane endpoints. Twenty-seven (27) rats were allotted in 4 groups and treated with L-Dopa alone (6 mg kg^{-1} + benserazide 15 mg kg^{-1}, s.c., n=6), or L-Dopa combined with CCG-203920 (10 mg kg^{-1}, i.p., n=7), AT-403 (0.03 mg kg^{-1}, n=7) or CCG-203920 + AT-403 (n=7). In combination studies, CCG-203920 was administered first, followed 5 min later by AT-403 and 10 min later by L-Dopa. Western blot analysis was carried out as previously described (Arcuri *et al.*, 2018; Paolone *et al.*, 2015). Thirty minutes after L-Dopa, rats were anaesthetized with isoflurane, sacrificed by decapitation and striata rapidly dissected and frozen in liquid nitrogen and stored at -80°C until analysis. In the study where RGS4 levels were analysed, seven additional dyskinetic rats (receiving last challenge of L-Dopa 24-48 hours earlier) were also included (L-Dopa OFF group). Tissues were homogenized in lysis buffer (SDS 1% buffer, protease inhibitor cocktail and phosphatase inhibitor cocktail) and centrifuged at 18000×g at 4°C for 15 min. Supernatants were collected, and protein levels were quantified using the Pierce™ BCA protein assay kit (Thermo Fisher Scientific, Cat# 23225). Samples were then stored at -80°C until use. Thirty micrograms of protein per sample were separated on a 4-12% gradient polyacrylamide precast gels (Bolt® 4-12% Bis-TrisPlus Gels, Life Technologies) in a Bolt® Mini Gel Tank apparatus (Life Technologies). Proteins were then transferred onto polyvinyldifluoride membrane, blocked for 60 min with 5% non-fat dry milk in 0.1% Tween20 Tris-buffered saline and incubated overnight at 4°C with anti-Thr202/Tyr204-phosphorylated ERK1/2 (pERK) rabbit monoclonal antibody (Merck Millipore, Cat# 05-797R, RRID:AB_1587016, 1:1000), anti-ERK1/2 (totERK) rabbit polyclonal antibody (Merck Millipore Cat# 06-182 RRID:AB_310068, 1:5000), anti-phospho-Ser845 GluR1 (pGluR1) rabbit polyclonal antibody (PhosphoSolutions, Cat# p1160-845

RRID:AB_2492128, 1:1000), antiGlutamate receptor 1 (totGluR1) rabbit polyclonal antibody (Merck Millipore Cat# AB1504 RRID:AB_2113602, 1:1000), anti-Tyrosine hydroxylase (TH) rabbit monoclonal antibody (Merck Millipore, Cat# AB152, RRID:AB_390204, 1:1000), anti-alpha Tubulin rabbit monoclonal antibody (Merck Millipore, Cat# 04-1117, RRID:AB_11213819, 1:25,000). Membranes were washed, then incubated 1 h at room temperature with horseradish peroxidase-linked secondary antibodies (Merck Millipore, Cat# 12-348, RRID:AB_390191, 1:2000). Immunoreactivity was visualized by enhanced chemiluminescence detection kit (Thermo Fisher Scientific, Cat# 32209), and images were acquired using the ChemiDoc MP System quantified using the Image Lab Software (Bio-Rad). Membranes were then stripped and re-probed with rabbit monoclonal anti-alpha Tubulin antibody (Merck Millipore, Cat# 04-1117, 1:50,000). Data were analyzed by densitometry, and the optical density of specific total ERK, total GluR1, RGS4 or TH bands was normalized to the corresponding tubulin levels. Optical density of specific pERK and pGluR1 bands were normalized on totERK and totGluR1 levels, respectively (Arcuri *et al.*, 2018; Paolone *et al.*, 2015). A molecular weight marker from Bio-Rad (Ca# 1610374) was used to identify the specific bands.

2.4 Data and analysis

The manuscript complies with BJP's recommendations and requirements on experimental design and analysis (Curtis *et al.*, 2018). Statistical analysis was undertaken only for studies where each group size was at least n=5 of independent values and statistical analysis was done on these independent values. A n=3 group size was adopted for studies on CCG-203920 specificity for RGS4 vs RGS19 presented in Supp Fig. 1. Group size was determined based on our previous studies with the protocols adopted (Arcuri *et al.*, 2018; Marti *et al.*, 2012; Paolone *et al.*, 2015; Papale *et al.*, 2016). All data were analyzed using GraphPad Prism 8.4.3 (GraphPad; LaJolla, CA, USA, RRID:SCR_002798). cAMP data in Fig. 1-3 were calculated

as percentage of SKF-38393 stimulation. Concentration-response curves for N/OFQ and AT-403 in cells co-transfected with NOP, NOP/RGS4 and NOP/RGS19 were fitted to non-linear least-square regression to the log (inhibitor) vs response (three parameters) in GraphPad Prism. Potency was expressed as pIC_{50} accompanied by 95% confidence interval in parenthesis. pIC50 and E_{max} values in Fig.1 were compared by the Student t-test, two-tailed for unpaired data. pERK data in striatal slices (Fig. 3) were analysed using a 3-way ANOVA followed by Bonferroni post hoc test. Immobility time and number of steps (Fig. 4) were expressed in absolute values and analysed using 2-way repeated measure (RM) ANOVA followed by the Tukey test. Dyskinesia values (Fig. 5A) were expressed as ALO score (frequency x amplitude) and were treated using two-way RM ANOVA followed by the Tukey test. Rotarod performance (Fig. 5B) was expressed as time on rod (in seconds) and was analysed using the Student t-test (two-tailed for unpaired data). Western blot values in Fig. 6-7 were analysed using the Student t-test, two-tailed for unpaired data, comparing the signal in the lesioned vs unlesioned striatum. RGS4 protein levels (Fig. 8) were expressed as a ratio to tubulin as housekeeper in absolute values (Fig. 8A) or as percentage of unlesioned striatum (Fig. 8B). Data in Fig. 8A were analysed using one-way ANOVA followed by the Newman-Keuls test whereas data in Fig. 8B, that did not pass the normality test, with the Kruskal-Wallis test for non-parametric ANOVA followed by the Dunn test. P values <0.05 were considered statistically significant. When parametric statistics was applied, the post-hoc tests were conducted only if F-value from ANOVA reached $p<0.05$ and there was no significant variance inhomogeneity. Overall, two outliers (one in figure 1 and another in figure 8) were excluded from data analysis and representation using the ROUT test implemented on the GraphPad Prism software. Outliers were indicated in figure legends.

2.5 Materials

AT-403 (2-(1-(1-((1s,4s)-4-isopropylcyclohexyl)piperidin-4-yl)-2-oxoindolin-3-yl)Nmethylacetamide) was synthesized by Dr NT Zaveri at Astraea Therapeutics (Mountain View, CA, USA) (Arcuri *et al.*, 2018). CCG-203920 (4-(2-(methoxyethyl-)-2-ethyl-1,2,4-thiadiazolidine-3,5-dione) was synthesized by the Medicinal Chemistry Core at Michigan State University (East Lansing, MI, USA). L-Dopa methyl ester hydrochloride and benserazide hydrochloride were purchased from Sigma-Aldrich (Milan, Italy). 6-OHDA hydrobromide and N/OFQ were purchased from Tocris Bioscience (Bristol, UK). The drug doses or concentrations indicated in text refer to the base form. U1079 antibody was a generous gift of Dr SM Mumby (University of Texas Southwestern, Dallas, TX, USA). AT-403 was dissolved in 2% CH3COOH 1M and 4% DMSO water, L-DOPA, benserazide and CCG-203920 were dissolved in saline, 6-OHDA was dissolved in saline with 0.02% ascorbic acid. N/OFQ and SKF-38393 were dissolved in water. LANCE Ultra cAMP assay was purchased from Perkin Elmer (Waltham, MA). The D1 receptor (Cat# DRD0100000), $G\alpha_s$ (Cat# GNA0SL0000), NOP (Cat# OPRL100000) plasmids were all purchased from cDNA Resource center (Bloomsburg, PA, USA).

2.6 Nomenclature of Targets and Ligands

Key protein targets and ligands in this article are hyperlinked to corresponding entries in http://www.guidetopharmacology.org, and are permanently archived in the Concise Guide to PHARMACOLOGY 2021/22: Introduction and Other Protein Targets (Alexander *et al.*, 2021b) and Concise Guide to PHARMACOLOGY 2021/22: G protein-coupled receptors (Alexander *et al.*, 2021a).

3. Results

3.1 In vitro experiments

3.1.1 RGS4 negatively modulates NOP receptor-driven inhibition of D1-stimulated cAMP production in HEK293T cells

The crosstalk between NOP and RGS4 was first investigated in HEK273 cells by measuring the inhibition of cAMP production stimulated by D1 receptor agonist SKF-38393 (40 nM) as a biochemical readout (Fig. 1). The NOP receptor endogenous ligand, N/OFQ, and the small molecule NOP agonist, AT-403, were tested in cells transfected with the NOP receptor alone or with RGS4. In NOP-transfected cells (Fig.1), N/OFQ inhibited cAMP production in a concentration-dependent manner. N/OFQ showed a pIC_{50} of 9.43 (10.15-8.70) and a maximal inhibition of cAMP production (E_{max}) of 61%. Co-transfection of RGS4 with the NOP receptor caused a rightward shift of the concentration-response curve of N/OFQ (Fig.1A) with a significant reduction of pIC_{50} to 8.66 (9.62-7.69) (df=12, t=3.56) and E_{max} to 45%. To investigate whether the NOP receptor might be regulated by other RGS proteins, the response of N/OFQ in the presence of RGS19 was assessed (Fig. 1A). In fact, RGS19 is structurally very similar to RGS4 and was reported to interact with the NOP receptor (Xie *et al.*, 2005). When NOP receptor and RGS19 were co-transfected, the N/OFQ curve was shifted to the right (Fig.1), with a significant reduction of N/OFQ potency (pIC_{50} 8.71, 9.88-7.55) (df=12, t=3.093) and a non-significant reduction of N/OFQ E_{max} to 39%.

Whether RGS4 and RGS19 also modulate the effect of AT-403 was next investigated. AT-403 (Fig. 1B) inhibited the D1-stimulated cAMP production in a concentration-dependent manner, showing slightly higher potency (pIC_{50}=9.92, 10.78-9.06) and efficacy (75%) than N/OFQ. RGS4 co-transfection caused a rightward shift of the AT-403 curve (Fig. 2), with a significant reduction of potency (pIC_{50}=9.22, 9.77-8.66) (df=11, t=2.71) and efficacy (50%, df=11 t=3.79). Co-transfection of RGS19 also shifted to the right the AT-403 curve (Fig. 1B), leading to a significant reduction (df=11 t=4.10) of AT-403 potency (pIC_{50}=8.93, 9.92-7.93) and efficacy (44%, df=11, t=3.24).

3.1.2 CCG-203920 potentiated the NOP response in rat primary striatal neurons

To investigate the occurrence of a RGS4-NOP receptor interaction in native tissues, the impact of pharmacological inhibition of RGS4 on NOP responses was investigated using the experimental RGS4 chemical probe CCG-203920 in individual medium sized spiny neurons (MSNs) in primary cultures of the E14 rat striatum (Fig. 2). CCG-203920 was chosen as the most selective agent for RGS4 vs RGS19 which is also able to modulate NOP effects in HEK-293 cells. Like its close derivative CCG-203769 (compound 11b, while CCG-203920 is compound 13 in (Turner *et al.*, 2012)), CCG-203920 acts most potently on RGS4 of all RGS proteins tested. Indeed, a preliminary analysis revealed that CCG-203920 is nearly 100-fold selective for RGS4 vs RGS19 (Supp. Fig. 1) whereas CCG-203769 is 8-fold selective for RGS4 vs RGS19 (Blazer *et al.*, 2015). Individual MSNs were identified using immunocytochemistry for DARPP-32 which is a well-known marker of MSNs (Ouimet *et al.*, 1984) and were co-stained for cAMP. cAMP accumulation was then measured in DARPP32+ neurons stimulated with the D1 receptor agonist SKF-38393 (100 μM) combined with increasing concentrations of N/OFQ, in the presence or the absence of CCG-203920 (100 nM). SKF-38393 caused an 83% increase of cAMP levels that was not significantly affected by CCG-203920 (Fig. 2A). N/OFQ inhibited the stimulation induced by SKF-38393 in a concentration-dependent manner with an pIC_{50} of 10.81 (11.36-10.26) and a 70% maximal inhibition of cAMP levels (Fig. 2B). CCG-203920 caused a leftward shift of N/OFQ pIC50 to 11.55 (12.43-10.67), without changing N/OFQ efficacy (Fig. 2B).

3.1.3 CCG-203920 potentiated NOP response in mouse striatal slices

Relying on the well-established NOP receptor inhibitory activity on D1 signaling (Olianas *et al.*, 2008), we next investigated whether RGS4 could affect the AT-403 mediated inhibition of the SKF-38393-induced ERK-positive cell number in slices of mouse striatum (Fig. 3). Application of the D1 receptor agonist SKF-38393 (100 μM) (Arcuri *et al.*, 2018; Fasano *et*

al., 2009; Marti *et al.*, 2012) to striatal slices of naïve mice caused an approximately four-fold increase in the number of pERK immunoreactive cells over basal (three-way ANOVA, $F_{1,42}$=213.909; Fig. 3). AT-403 alone (30 nM) had no effect on basal pERK levels but reduced D1 receptor-mediated response by 56% (three-way ANOVA, $F_{1,42}$=102.746). CCG-203920, which was ineffective alone, significantly potentiated the effects of AT-403 (three-way ANOVA, $F_{1,42}$=9.222). In fact, when co-applied with CCG-203920, AT-403 fully inhibited D1 stimulation.

3.2 In vivo experiments

3.2.1 CCG-203920 targets RGS4 in vivo

To confirm the RGS4 selectivity of CCG-20920 in vivo, the neuroleptic-induced akinesia/catalepsy model was used since we previously reported that the RGS4 inhibitor CCG-203769 reversed raclopride-induced akinesia in mice (Blazer *et al.*, 2015). $RGS4^{-/-}$ mice were slightly hypokinetic at baseline, showing >2-fold greater immobility time in the bar test (14.45 ± 1.40 s, n=20) and 40% reduced stepping activity in the drag test (6.59 ± 0.56 steps, n=20) compared to controls (5.7 ± 0.48 s and 10.08 ± 0.45 steps, respectively; n=20 each). Two-way ANOVA revealed that raclopride caused a prolonged and marked increase of the immobility time (time $F_{3,108}$=117.3, p<0.0001; treatment $F_{3,36}$=11.34, p<0.0001, time X treatment interaction $F_{9,108}$=6.35, p<0.0001) and a reduction of stepping activity (time $F_{3,95}$=67.50, p<0.0001; treatment $F_{3.36}$=18.95, p<0.0001, time X treatment interaction $F_{9,108}$=4.09, p=0.0002) in both wild-type and $RGS4^{-/-}$ mice (Fig. 4). CCG-203920 administration significantly reversed raclopride-induced hypokinesia in wild-type animals but was ineffective in $RGS4^{-/-}$ mice, suggesting RGS4 targeting at this dose.

3.2.2 CCG-203920 extended the antidyskinetic effect of AT-403

In a previous study, we described the dose-dependent antidyskinetic effect of AT-403 in the 6-OHDA rat model of LID in vivo (Arcuri *et al.*, 2018). At the highest dose tested AT-403

(0.1 mg kg^{-1}) exerted strong sedative effects that overlapped the antidyskinetic effect. Conversely, at the dose of 0.03 mg kg^{-1}, AT-403 exerted a mild and transient antidyskinetic effect in the absence of sedation. Here, in the same model, to improve the antidyskinetic effect of this AT-403 dose, we challenged AT-403 (0.03 mg kg^{-1} s.c.) with L-Dopa (6 mg kg^{-1} + benserazide 15 mg kg^{-1} s.c.) in the presence and in the absence of CCG-203920 10 mg kg^{-1} (Fig. 5A). AT-403 alone delayed the onset of AIMs by 40 min, without affecting the overall duration and severity of the response. Co-administration of CCG-203920 caused a further 20 min delay in AIM appearance, without significantly affecting the overall response to AT-403 (Fig. 5A), suggesting that RGS4 blockade potentiates NOP agonist induced antidyskinetic effects (significant effect of time $F_{8,432}$=37.00, treatment $F_{3,432}$=6.86, and time x treatment interaction $F_{24,432}$=43.06).

3.2.3 CCG-203920 did not affect the improvement of rotarod performance ON L-Dopa induced by AT-403

To investigate whether CCG-203920 increased the sedative effects along with the antidyskinetic effect of AT-403, the rotarod performance was monitored before (baseline, OFF L-Dopa) and after L-Dopa administration in dyskinetic rats (Arcuri *et al.*, 2018; Marti *et al.*, 2012; Paolone *et al.*, 2015) (Fig. 5B). As expected, the time spent on the rod after L-Dopa administration was dramatically reduced compared to baseline due to dyskinetic movement appearance (-76%; df=10 t=4.075). When animals were pretreated with AT-403, the rotarod performance ON L-Dopa improved and no significant reduction with respect to baseline condition was observed (Fig. 5B). CCG-203920 administration did not worsen the motor promoting effect of AT-403, indicating RGS4 blockade did not potentiate AT-403-induced sedation.

3.2.4 CCG-203920 potentiated the AT-403 inhibition of ERK signaling in striatum

Aberrant D1 receptor transmission in direct pathway MSNs is associated with LID and leads to alterations in phosphorylating activity of several downstream kinases, such as PKA and DARPP-32 (Bastide *et al.*, 2015). A direct consequence of the hyperactivity of DARPP-32 is the increased phosphorylation of ERK1/2, a well-accepted correlate of LID in rodents (Pavon *et al.*, 2006; Santini *et al.*, 2007). In a previous study we showed that AT-403 (0.1 mg kg^{-1}) was able to normalize the L-Dopa induced pERK levels in the 6-OHDA lesioned, DA-depleted striatum (Arcuri *et al.*, 2018). In the present study, we investigated whether a lower dose of AT-403 (0.03 mg kg^{-1}) alone or in combination with CCG-203920 could normalize L-Dopa-induced increase of pERK in the striatum of dyskinetic rats (Fig. 6). As expected, LID was associated with a significant increase of pERK levels in the lesioned striatum relative to the unlesioned striatum (+47%; t=3.584 df=12), which was unaffected by pretreatment with AT-403 (+79%; t=2.261, df=10) or CCG-203920 (+117%; significance just above the threshold value t=1.947, df=10, p=0.08; Fig. 6A). However, when L-Dopa was combined with CCG-203920 and AT-403, pERK levels did not rise in the lesioned striatum (Fig. 6A). Pharmacological treatments did not affect total protein levels (Fig. 6B), suggesting that the changes observed were due to the activation of the pathway and not protein expression.

3.2.5 AT-403 inhibited D1 receptor-stimulated pGluR1 phosphorylation in striatum

The increase of pGluR1 levels is another biochemical correlate of LID in rodents (Santini *et al.*, 2007). GluR1 is a subunit of the glutamate AMPA receptor, which is physiologically phosphorylated by PKA activated by dopamine via D1 receptors. We therefore investigated whether CCG-203920 potentiates the ability of AT-403 (0.03 mg kg^{-1}) to modulate pGluR1 levels. As expected, L-Dopa elevated pGluR1 levels in the lesioned stratum (+52%; t=2.272, df=12; Fig. 7A). However, in contrast to the effect on ERK, AT-403 alone was able to normalize pGluR1 levels (Fig. 7A), in line with the well-known inhibitory influence of NOP

receptors over canonical D1 signaling. CCG-203920 did not alter the L-Dopa induced increase (+52%; t=2.239, df=10) or the AT-403-driven normalization of pGluR1 levels. Again, neither treatment affected total protein amounts (Fig. 7B).

3.2.6 Striatal RGS4 levels were modulated by DA depletion and L-Dopa treatment

To investigate whether RGS4 inhibition corrects a plastic adaptation of RGS4 occurring as a consequence of DA depletion and/or L-Dopa administration (Geurts *et al.*, 2003; Ko *et al.*, 2014), RGS4 levels were measured by Western analysis in the striatum of naïve, L-Dopa naïve 6-OHDA hemilesioned and dyskinetic rats (Fig. 8). In dyskinetic rats, RGS4 levels were measured both ON and OFF L-Dopa. The specificity of the antibody used was first confirmed in $RGS4^{-/-}$ mice (Supp Fig. 2). ANOVA revealed a strong effect of treatment ($F_{7,46}$=7.95). A marked decrease in RGS4 protein levels was found in both the lesioned (-64%) and unlesioned (-51%) striatum of 6-OHDA animals, when compared with respective naïve counterparts (Fig. 8A). If RGS4 levels were expressed as lesioned-to-unlesioned ratio, a significant reduction was detected in 6-OHDA hemilesioned rats compared to naive rats ($H_{3,20}$=13.73) (Fig. 8B). Chronic L-Dopa (OFF group) normalized the ratio. However, acute L-Dopa (ON group) reversed it, causing a 44% increase of RGS4 levels in the lesioned striatum. This suggests that RGS4 is rapidly upregulated in the lesioned striatum of dyskinetic animals following acute stimulation of aberrant D1 receptor signaling by L-Dopa.

4. Discussion and conclusions

The present study provides strong evidence that RGS4 inhibits NOP receptor responses in vitro. Moreover, this study demonstrates that pharmacological inhibition of RGS4 potentiates the ability of a NOP agonist to attenuate LID and its neurochemical correlates in vivo, without worsening its sedative properties. These data point to a functional RGS4-NOP receptor interaction, and add to previous reports that RGS4 fine-tunes opioid receptor

signaling and behaviors (Dripps *et al.*, 2017; Han *et al.*, 2010; Stratinaki *et al.*, 2013; Xie *et al.*, 2005). In fact, RGS4 negatively regulated reward and physical dependence induced by the MOP receptor preferential agonist morphine but did not affect morphine-induced analgesia or tolerance (Han *et al.*, 2010). RGS4 also differentially modulated DOP receptor-mediated behavioral outcomes in mice, since genetic deletion of RGS4 as well as acute pharmacological inhibition of RGS4 with CCG-203769, increased SNC80-induced antinociception and antihyperalgesia, but did not affect the pro-convulsant action of this DOP agonist (Dripps *et al.*, 2017; Stratinaki *et al.*, 2013).

The interaction between RGS4 and NOP receptor was originally evaluated in COS-7 cells transfected with a dual-expression plasmid containing RGS4 and each of the opioid receptor subtypes (Xie *et al.*, 2005). In that study a single concentration of N/OFQ was tested, which was poorly modulated by RGS4. In fact, RGS4 increased by 28% N/OFQ GTPase activity but left unaffected N/OFQ inhibition of forskolin-induced cAMP levels. In the present study in HEK293T cells, RGS4 did not affect N/OFQ efficacy but significantly reduced its potency. Moreover, it reduced both the efficacy and potency of the potent and selective small molecule agonist AT-403. In NOP-transfected HEK293T cells, N/OFQ and AT-403 inhibited the D1-stimulated cAMP production, a Gi/o protein-mediated intracellular function (Feng *et al.*, 2017) with similar potencies (9.43 and 9.92, respectively).These values are consistent with those reported for N/OFQ and AT-403 in the [^{35}S]GTPγS and calcium mobilization assays (Ferrari *et al.*, 2017) confirming that AT-403 is a potent full agonist at the NOP receptor. The rightward shift of N/OFQ and AT-403 curves and the reduction of AT-403 efficacy in the presence of RGS4 suggests that RGS4 negatively couples to Gi/o to inhibit NOP receptor signaling. However, this effect is shared by another RGS protein, RGS19, functionally very close to RGS4, which was reported to negatively modulate NOP receptor signaling in vitro (Xie *et al.*, 2005). Interestingly, RGS19 reduced the efficacy of AT-403, but showed only a

trend for reduction of N/OFQ efficacy. Thus, RGS4 and RGS19 seem to modulate more efficiently the efficacy of AT-403 than of N/OFQ. This could be due to the different modes of interaction and activation of the NOP receptor by the endogenous ligand N/OFQ versus a small-molecule nonpeptidic ligand like AT-403.

The occurrence of a RGS4-NOP functional interaction was confirmed in native systems, i.e. striatal primary neurons and striatal slices, using an experimental RGS4 chemical probe to block the endogenous activity of RGS4. Primary striatal neurons express both RGS4 and NOP (Buzas *et al.*, 1998; Runne *et al.*, 2008) and the two functionally interact to modulate D1 receptor evoked responses since the highly RGS4-selective CCG-203920 increased N/OFQ potency in inhibiting D1-stimulated cAMP levels. This interaction occurs in DARRP32-positive, likely GABAergic, neurons indicating this interaction is not an artifact of protein overexpression in HEK273 cells but is endogenously active and physiologically relevant. This interaction occurs not only in developing tissues in rats but also in adult mice. We previously demonstrated that N/OFQ and AT-403 inhibited the increase of ERK-positive striatal neurons (likely MSNs) induced by D1 receptor agonist SKF-38393 in striatal slices (Arcuri *et al.*, 2018; Marti *et al.*, 2012), a biochemical predictor of antidyskinetic activity. In this model, we now show that CCG-203920 potentiates the effect of a submaximal dose of AT-403 without affecting the D1 response alone. Consistently, CCG-203920 potentiated the antidyskinetic effect of AT-403, significantly extending the delay in AIM onset induced by AT-403. Since this effect was not accompanied by the worsening of the positive effect of AT-403 on rotarod performance, it is likely due a true potentiation of its antidyskinetic properties. Since we show that the same dose of CCG-203920 reversed raclopride-induced akinesia in mice through selective interaction with RGS4, we are confident that also the antidyskinetic effect of CCG-20920 is mediated by RGS4 targeting. To confirm that the effect of CCG-203920 is truly mediated by interference with the molecular pathways underlying LID, CCG-

203920 potentiated the inhibition of ERK phosphorylation induced by AT-403. LID is characterized by aberrant enhancement of Gα and Gβγ signaling pathways downstream of the D1 receptor, such as the cAMP/PKA and MAPK cascades (Santini *et al.*, 2007). Specifically, the increased activity along the canonical and non-canonical D1 pathways leads to the phosphorylation of several downstream effectors in striatal direct pathway MSNs, such as the GluR1 subunit of glutamate AMPA receptor and ERK (Pavon *et al.*, 2006; Santini *et al.*, 2007) . We previously reported that a dose of AT-403 as high as 0.1 mg kg^{-1} normalized pERK levels and blunted LID (Arcuri *et al.*, 2018). We now report that a 3-fold lower dose, ineffective alone, normalized pERK levels when combined with the experimental RGS4 chemical probe CCG-203920, confirming that RGS4 blockade potentiates the ability of a NOP receptor agonist to modulate MAPK pathway changes underlying LID. As far as pGluR1 levels are concerned, AT-403 alone fully inhibited the rise of pGluR1 associated with dyskinesia, which might have precluded further inhibition by CCG-203920. Overall, these data indicate that RGS4 blockade improves the antidyskinetic effect induced by a NOP receptor agonist and the underlying signaling pathways, without amplifying its sedative effects. This suggests that as for δ opioid receptor agonists (Dripps *et al.*, 2017), RGS4 blockade might differentially impact NOP behaviors, and perhaps widen the therapeutic window between sedation and pharmacodynamic effects of potent NOP agonists like AT-403.

Interestingly, previous studies indicated the involvement of RGS4 in the pathogenesis of LID, showing that RGS4 blockade induced therapeutic antidyskinetic effects (Ko *et al.*, 2014; Shen *et al.*, 2015). Specifically, chronic treatment with antisense oligonucleotides targeting RGS4 reduced AIM development during L-Dopa priming in a rat model of LID (Ko *et al.*, 2014). Pharmacological blockade of RGS4 is expected to affect GPCRs other than the NOP receptor, inducing off-target effects in brain or neuronal populations not involved in LID. To

confirm that an RGS4 inhibitor would selectively target and correct a pathological condition, we show that striatal RGS4 level are reduced after DA depletion and rapidly upregulated after L-Dopa administration and dyskinesia onset. This further supports the rationale for therapeutic application of RGS4 inhibitors in LID therapy. Our data confirm previous evidence of reduction of RGS4 expression in DA-depleted animals (Geurts *et al.*, 2003; Ko *et al.*, 2014). More specifically, they nicely complement an ex-vivo study in 6-OHDA hemilesioned dyskinetic rats (Ko *et al.*, 2014), where RGS4 expression was found to be reduced in the lesioned striatum after DA depletion and increased following chronic L-Dopa treatment, the increase being more marked at 1 hour (i.e. ON L-Dopa) than at 24 hours (i.e. OFF L-Dopa) after L-Dopa administration. Surprisingly, however, our study also revealed a reduction in the unlesioned striatum, suggesting a powerful influence of the cortico-basal ganglia-thalamo-cortical loop and/or cross-striatal dopaminergic projections over RGS4 levels.

In conclusion, we provide strong evidence of a NOP-RGS4 receptor interaction in a cell line and in native tissues and its relevance for the therapy of LID. CCG-203920 potentiated the antidyskinetic effect of NOP agonists without worsening its primary sedative/hypolocomotor properties, possibly preventing the effects resulting from up-regulation of RGS4 induced by L-DOPA in striatum. RGS4 plays an important role in regulating striatal functions and plasticity under parkinsonian conditions (Lerner *et al.*, 2012; Shen *et al.*, 2015). The present study confirms the role of RGS4 in LID (Ko *et al.*, 2014; Shen *et al.*, 2015) and lends support to the therapeutic potential of RGS4 inhibitors in the therapy of neuropsychiatric disorders (Ahlers-Dannen *et al.*, 2020).

Declaration of transparency and scientific rigour

This Declaration acknowledges that this paper adheres to the principles for transparent reporting and scientific rigour of preclinical research as stated in the BJP guidelines for Design and Analysis, and Animal Experimentation, and as recommended by funding agencies, publishers and other organisations engaged with supporting research.

References

Ahlers-Dannen KE, Spicer MM, Fisher RA (2020). RGS Proteins as Critical Regulators of Motor Function and Their Implications in Parkinson's Disease. *Mol Pharmacol* **98**(6)**:** 730-738.

Alexander SP, Christopoulos A, Davenport AP, Kelly E, Mathie A, Peters JA*, et al.* (2021a). THE CONCISE GUIDE TO PHARMACOLOGY 2021/22: G protein-coupled receptors. *Br J Pharmacol* **178 Suppl 1:** S27-S156.

Alexander SP, Kelly E, Mathie A, Peters JA, Veale EL, Armstrong JF*, et al.* (2021b). THE CONCISE GUIDE TO PHARMACOLOGY 2021/22: Introduction and Other Protein Targets. *Br J Pharmacol* **178 Suppl 1:** S1-S26.

Alexander SPH, Roberts RE, Broughton BRS, Sobey CG, George CH, Stanford SC*, et al.* (2018). Goals and practicalities of immunoblotting and immunohistochemistry: A guide for submission to the British Journal of Pharmacology. *Br J Pharmacol* **175**(3)**:** 407-411.

Arcuri L, Novello S, Frassineti M, Mercatelli D, Pisano CA, Morella I*, et al.* (2018). Anti-Parkinsonian and anti-dyskinetic profiles of two novel potent and selective nociceptin/orphanin FQ receptor agonists. *Br J Pharmacol* **175**(5)**:** 782-796.

Bastide MF, Meissner WG, Picconi B, Fasano S, Fernagut PO, Feyder M*, et al.* (2015). Pathophysiology of L-dopa-induced motor and non-motor complications in Parkinson's disease. *Prog Neurobiol*.

Berman DM, Wilkie TM, Gilman AG (1996). GAIP and RGS4 are GTPase-activating proteins for the Gi subfamily of G protein alpha subunits. *Cell* **86**(3)**:** 445-452.

Blazer LL, Storaska AJ, Jutkiewicz EM, Turner EM, Calcagno M, Wade SM*, et al.* (2015). Selectivity and anti-Parkinson's potential of thiadiazolidinone RGS4 inhibitors. *ACS chemical neuroscience* **6**(6)**:** 911-919.

Brugnoli A, Pisano CA, Morari M (2020). Striatal and nigral muscarinic type 1 and type 4 receptors modulate levodopa-induced dyskinesia and striato-nigral pathway activation in 6-hydroxydopamine hemilesioned rats. *Neurobiol Dis* **144:** 105044.

Buzas B, Rosenberger J, Cox BM (1998). Activity and cyclic AMP-dependent regulation of nociceptin/orphanin FQ gene expression in primary neuronal and astrocyte cultures. *J Neurochem* **71**(2)**:** 556-563.

Cenci MA, Crossman AR (2018). Animal models of l-dopa-induced dyskinesia in Parkinson's disease. *Mov Disord* **33**(6)**:** 889-899.

Cenci MA, Lee CS, Bjorklund A (1998). L-DOPA-induced dyskinesia in the rat is associated with striatal overexpression of prodynorphin- and glutamic acid decarboxylase mRNA. *Eur J Neurosci* **10**(8)**:** 2694-2706.

Cenci MA, Lundblad M (2007). Ratings of L-DOPA-induced dyskinesia in the unilateral 6-OHDA lesion model of Parkinson's disease in rats and mice. *Curr Protoc Neurosci* **Chapter 9:** Unit 9 25.

Cifelli C, Rose RA, Zhang H, Voigtlaender-Bolz J, Bolz SS, Backx PH*, et al.* (2008). RGS4 regulates parasympathetic signaling and heart rate control in the sinoatrial node. *Circ Res* **103**(5)**:** 527-535.

Curtis MJ, Alexander S, Cirino G, Docherty JR, George CH, Giembycz MA*, et al.* (2018). Experimental design and analysis and their reporting II: updated and simplified guidance for authors and peer reviewers. *Br J Pharmacol* **175**(7)**:** 987-993.

Dripps IJ, Wang Q, Neubig RR, Rice KC, Traynor JR, Jutkiewicz EM (2017). The role of regulator of G protein signaling 4 in delta-opioid receptor-mediated behaviors. *Psychopharmacology (Berl)* **234**(1)**:** 29-39.

Duty S, Jenner P (2011). Animal models of Parkinson's disease: a source of novel treatments and clues to the cause of the disease. *Br J Pharmacol* **164**(4)**:** 1357-1391.

Ebert PJ, Campbell DB, Levitt P (2006). Bacterial artificial chromosome transgenic analysis of dynamic expression patterns of regulator of G-protein signaling 4 during development. II. Subcortical regions. *Neuroscience* **142**(4)**:** 1163-1181.

Fasano S, D'Antoni A, Orban PC, Valjent E, Putignano E, Vara H*, et al.* (2009). Ras-guanine nucleotide-releasing factor 1 (Ras-GRF1) controls activation of extracellular signal-regulated kinase (ERK) signaling in the striatum and long-term behavioral responses to cocaine. *Biol Psychiatry* **66**(8)**:** 758-768.

Feng H, Sjogren B, Karaj B, Shaw V, Gezer A, Neubig RR (2017). Movement disorder in GNAO1 encephalopathy associated with gain-of-function mutations. *Neurology* **89**(8)**:** 762-770.

Ferrari F, Malfacini D, Journigan BV, Bird MF, Trapella C, Guerrini R*, et al.* (2017). In vitro pharmacological characterization of a novel unbiased NOP receptor-selective nonpeptide agonist AT-403. *Pharmacology research & perspectives* **5**(4).

Garzon J, Rodriguez-Diaz M, Lopez-Fando A, Sanchez-Blazquez P (2001). RGS9 proteins facilitate acute tolerance to mu-opioid effects. *Eur J Neurosci* **13**(4)**:** 801-811.

Geurts M, Maloteaux JM, Hermans E (2003). Altered expression of regulators of G-protein signaling (RGS) mRNAs in the striatum of rats undergoing dopamine depletion. *Biochem Pharmacol* **66**(7)**:** 1163-1170.

Gold SJ, Ni YG, Dohlman HG, Nestler EJ (1997). Regulators of G-protein signaling (RGS) proteins: region-specific expression of nine subtypes in rat brain. *J Neurosci* **17**(20)**:** 8024-8037.

Gross JD, Kaski SW, Schmidt KT, Cogan ES, Boyt KM, Wix K*, et al.* (2019). Role of RGS12 in the differential regulation of kappa opioid receptor-dependent signaling and behavior. *Neuropsychopharmacology* **44**(10)**:** 1728-1741.

Han MH, Renthal W, Ring RH, Rahman Z, Psifogeorgou K, Howland D*, et al.* (2010). Brain region specific actions of regulator of G protein signaling 4 oppose morphine reward and dependence but promote analgesia. *Biol Psychiatry* **67**(8)**:** 761-769.

Jutkiewicz EM, Rice KC, Traynor JR, Woods JH (2005). Separation of the convulsions and antidepressant-like effects produced by the delta-opioid agonist SNC80 in rats. *Psychopharmacology (Berl)* **182**(4)**:** 588-596.

Kimple AJ, Bosch DE, Giguere PM, Siderovski DP (2011). Regulators of G-protein signaling and their Galpha substrates: promises and challenges in their use as drug discovery targets. *Pharmacol Rev* **63**(3)**:** 728-749.

Ko WK, Martin-Negrier ML, Bezard E, Crossman AR, Ravenscroft P (2014). RGS4 is involved in the generation of abnormal involuntary movements in the unilateral 6-OHDA-lesioned rat model of Parkinson's disease. *Neurobiol Dis* **70:** 138-148.

Lerner TN, Kreitzer AC (2012). RGS4 is required for dopaminergic control of striatal LTD and susceptibility to parkinsonian motor deficits. *Neuron* **73**(2)**:** 347-359.

Lilley E, Stanford SC, Kendall DE, Alexander SPH, Cirino G, Docherty JR*, et al.* (2020). ARRIVE 2.0 and the British Journal of Pharmacology: Updated guidance for 2020. *Br J Pharmacol* **177**(16)**:** 3611-3616.

Marti M, Mela F, Fantin M, Zucchini S, Brown JM, Witta J*, et al.* (2005). Blockade of nociceptin/orphanin FQ transmission attenuates symptoms and neurodegeneration associated with Parkinson's disease. *J Neurosci* **25**(42)**:** 9591-9601.

Marti M, Mela F, Guerrini R, Calo G, Bianchi C, Morari M (2004). Blockade of nociceptin/orphanin FQ transmission in rat substantia nigra reverses haloperidol-induced akinesia and normalizes nigral glutamate release. *J Neurochem* **91**(6)**:** 1501-1504.

Marti M, Rodi D, Li Q, Guerrini R, Fasano S, Morella I*, et al.* (2012). Nociceptin/orphanin FQ receptor agonists attenuate L-DOPA-induced dyskinesias. *J Neurosci* **32**(46)**:** 16106-16119.

Mercatelli D, Bezard E, Eleopra R, Zaveri NT, Morari M (2020). Managing Parkinson's disease: moving ON with NOP. *Br J Pharmacol* **177**(1)**:** 28-47.

Neal CR, Jr., Mansour A, Reinscheid R, Nothacker HP, Civelli O, Akil H*, et al.* (1999). Opioid receptor-like (ORL1) receptor distribution in the rat central nervous system: comparison of ORL1 receptor mRNA expression with (125)I-[(14)Tyr]-orphanin FQ binding. *J Comp Neurol* **412**(4)**:** 563-605.

Olianas MC, Dedoni S, Boi M, Onali P (2008). Activation of nociceptin/orphanin FQ-NOP receptor system inhibits tyrosine hydroxylase phosphorylation, dopamine synthesis, and dopamine D(1) receptor signaling in rat nucleus accumbens and dorsal striatum. *J Neurochem* **107**(2)**:** 544-556.

Ouimet CC, Miller PE, Hemmings HC, Jr., Walaas SI, Greengard P (1984). DARPP-32, a dopamine- and adenosine 3':5'-monophosphate-regulated phosphoprotein enriched in dopamine-innervated brain regions. III. Immunocytochemical localization. *J Neurosci* **4**(1)**:** 111-124.

Paolone G, Brugnoli A, Arcuri L, Mercatelli D, Morari M (2015). Eltoprazine prevents levodopa-induced dyskinesias by reducing striatal glutamate and direct pathway activity. *Mov Disord* **30**(13)**:** 1728-1738.

Papale A, Morella IM, Indrigo MT, Bernardi RE, Marrone L, Marchisella F*, et al.* (2016). Impairment of cocaine-mediated behaviours in mice by clinically relevant Ras-ERK inhibitors. *eLife* **5**.

Pavon N, Martin AB, Mendialdua A, Moratalla R (2006). ERK phosphorylation and FosB expression are associated with L-DOPA-induced dyskinesia in hemiparkinsonian mice. *Biol Psychiatry* **59**(1)**:** 64-74.

Paxinos G, Watson C (1986). *The rat brain in stereotaxic coordinates*. 2nd edn. Academic Press: Sydney ; Orlando.

Percie du Sert N, Hurst V, Ahluwalia A, Alam S, Avey MT, Baker M*, et al.* (2020). The ARRIVE guidelines 2.0: Updated guidelines for reporting animal research. *Br J Pharmacol* **177**(16)**:** 3617-3624.

Pisanò CA, Brugnoli A, Novello S, Caccia C, Keywood C, Melloni E*, et al.* (2020). Safinamide inhibits in vivo glutamate release in a rat model of Parkinson's disease. *Neuropharmacology* **167**.

Psifogeorgou K, Papakosta P, Russo SJ, Neve RL, Kardassis D, Gold SJ*, et al.* (2007). RGS9-2 is a negative modulator of mu-opioid receptor function. *J Neurochem* **103**(2)**:** 617-625.

Runne H, Regulier E, Kuhn A, Zala D, Gokce O, Perrin V*, et al.* (2008). Dysregulation of gene expression in primary neuron models of Huntington's disease shows that polyglutamine-related effects on the striatal transcriptome may not be dependent on brain circuitry. *J Neurosci* **28**(39)**:** 9723-9731.

Sakloth F, Polizu C, Bertherat F, Zachariou V (2020). Regulators of G protein signaling in analgesia and addiction. *Mol Pharmacol*.

Santini E, Valjent E, Usiello A, Carta M, Borgkvist A, Girault JA*, et al.* (2007). Critical involvement of cAMP/DARPP-32 and extracellular signal-regulated protein kinase signaling in L-DOPA-induced dyskinesia. *J Neurosci* **27**(26)**:** 6995-7005.

Schmidt ER, Morello F, Pasterkamp RJ (2012). Dissection and culture of mouse dopaminergic and striatal explants in three-dimensional collagen matrix assays. *Journal of visualized experiments : JoVE*(61).

Schwarting RK, Huston JP (1996). The unilateral 6-hydroxydopamine lesion model in behavioral brain research. Analysis of functional deficits, recovery and treatments. *Prog Neurobiol* **50**(2-3)**:** 275-331.

Senese NB, Kandasamy R, Kochan KE, Traynor JR (2020). Regulator of G-Protein Signaling (RGS) Protein Modulation of Opioid Receptor Signaling as a Potential Target for Pain Management. *Frontiers in molecular neuroscience* **13:** 5.

Shen W, Plotkin JL, Francardo V, Ko WK, Xie Z, Li Q*, et al.* (2015). M4 Muscarinic Receptor Signaling Ameliorates Striatal Plasticity Deficits in Models of L-DOPA-Induced Dyskinesia. *Neuron* **88**(4)**:** 762-773.

Sjogren B (2017). The evolution of regulators of G protein signalling proteins as drug targets - 20 years in the making: IUPHAR Review 21. *Br J Pharmacol* **174**(6)**:** 427-437.

Stratinaki M, Varidaki A, Mitsi V, Ghose S, Magida J, Dias C*, et al.* (2013). Regulator of G protein signaling 4 [corrected] is a crucial modulator of antidepressant drug action in depression and neuropathic pain models. *Proc Natl Acad Sci U S A* **110**(20)**:** 8254-8259.

Tesmer JJ, Berman DM, Gilman AG, Sprang SR (1997). Structure of RGS4 bound to AlF4--activated G(i alpha1): stabilization of the transition state for GTP hydrolysis. *Cell* **89**(2)**:** 251-261.

Toll L, Bruchas MR, Calo G, Cox BM, Zaveri NT (2016). Nociceptin/Orphanin FQ Receptor Structure, Signaling, Ligands, Functions, and Interactions with Opioid Systems. *Pharmacol Rev* **68**(2)**:** 419-457.

Traynor J (2012). mu-Opioid receptors and regulators of G protein signaling (RGS) proteins: from a symposium on new concepts in mu-opioid pharmacology. *Drug Alcohol Depend* **121**(3)**:** 173-180.

Traynor JR, Neubig RR (2005). Regulators of G protein signaling & drugs of abuse. *Mol Interv* **5**(1)**:** 30-41.

Turner EM, Blazer LL, Neubig RR, Husbands SM (2012). Small Molecule Inhibitors of Regulator of G Protein Signalling (RGS) Proteins. *ACS medicinal chemistry letters* **3**(2)**:** 146-150.

Viaro R, Sanchez-Pernaute R, Marti M, Trapella C, Isacson O, Morari M (2008). Nociceptin/orphanin FQ receptor blockade attenuates MPTP-induced parkinsonism. *Neurobiol Dis* **30**(3)**:** 430-438.

Xie GX, Yanagisawa Y, Ito E, Maruyama K, Han X, Kim KJ*, et al.* (2005). N-terminally truncated variant of the mouse GAIP/RGS19 lacks selectivity of full-length GAIP/RGS19 protein in regulating ORL1 receptor signaling. *J Mol Biol* **353**(5)**:** 1081-1092.

Zachariou V, Georgescu D, Sanchez N, Rahman Z, DiLeone R, Berton O*, et al.* (2003). Essential role for RGS9 in opiate action. *Proc Natl Acad Sci U S A* **100**(23)**:** 13656-13661.

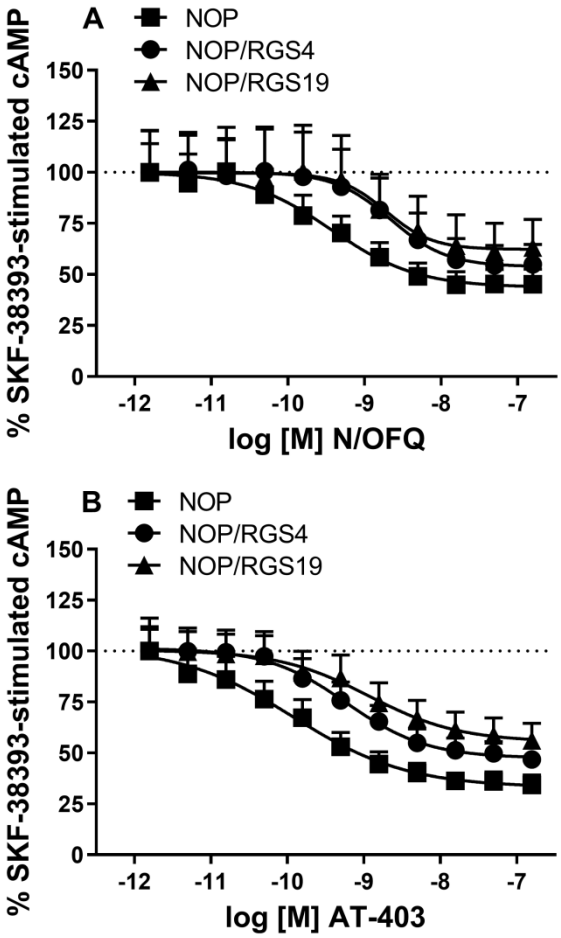

Figure 1. RGS4 and RGS19 reduced the NOP receptor agonist ability to attenuate the accumulation of cAMP triggered by D1 receptor agonist in cells. HEK-293T cells were transfected with plasmids for the D1 and NOP receptors, $G\alpha_s$ with or without RGS4 or RGS19 as described in Materials and Methods. They were then stimulated with the D1 receptor agonist SKF-38393 at 40 nM. Concentration–response curves of the NOP receptor agonists N/OFQ (0.001 nM-1 μM. A) and AT-403 (0.001 nM- 1 μM; B). Data are mean ± SEM of n=7 experiments per group (one outlier in the NOP group of panel B).

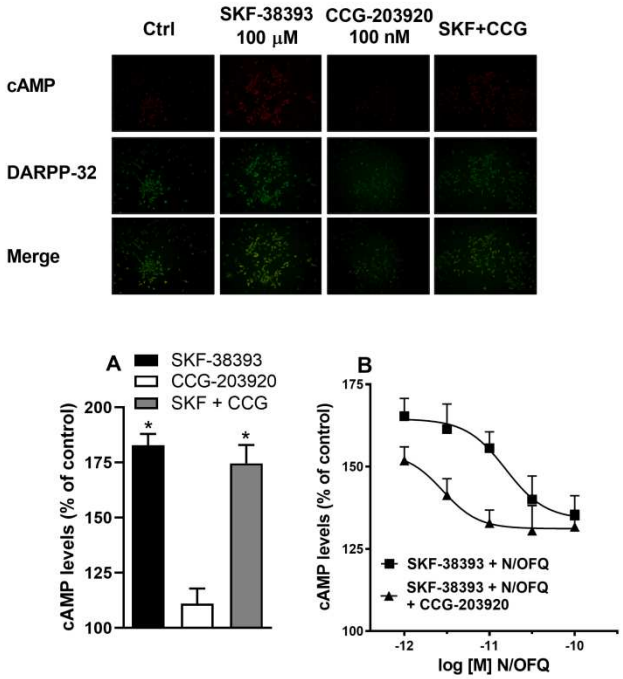

Figure 2. RGS4 reduced the NOP receptor agonist ability to attenuate the accumulation of cAMP triggered by D1 receptor agonist in DARPP-32+ striatal primary neurons. DARPP-32 is a marker of MSNs. Neurons were treated with the D1 receptor agonist SKF-38393 (100 μM) and the NOP receptor agonist N/OFQ (0.01-1 nM), in the presence or the absence of the experimental RGS4 chemical probe CCG-203920 (100 nM). A. Primary effects of SKF-38393, CCG-203920 and their combination, with representative images (upper panels). B. Concentration-response curves of N/OFQ in the presence or the absence of CCG-203920. Data are mean ± SEM of n=8-10 experiments per group, namely N/OFQ 0.001 nM n=9, N/OFQ 0.003 n=8, N/OFQ 0.01 nM n=10, N/OFQ 0.03 nM n=10 (without CCG-203920) and n=8 (with CCG-203920), N/OFQ=0.1 nM (n=9). *$p<0.05$, different from CCG-203920 (one-way ANOVA followed by the Bonferroni post hoc test)

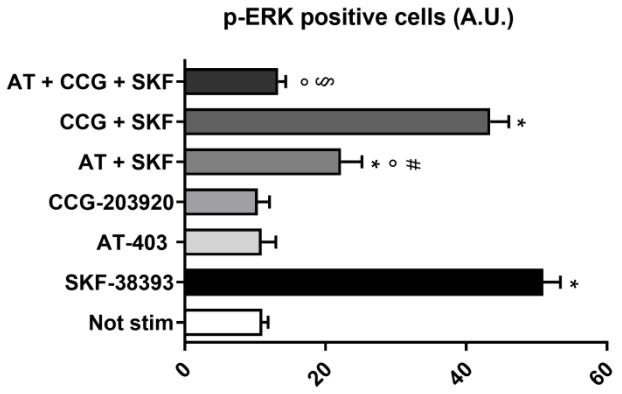

Figure 3. CCG-203920 potentiated the AT-403 driven inhibition of D1 receptor-stimulated ERK signalling in striatum. Number of ERK-positive cells in striatal slices of naïve mice following application of the D1 receptor agonist SKF-38393 (100 μM), the NOP receptor agonist AT-403 (30 nM) and the experimental RGS4 chemical probe CCG203920 (50 nM) alone and in combination. Data are mean ± SEM of n=7 mice per group. *p< 0.05, different from unstimulated vehicle; °p<0.05, different from SKF-38393 alone; # p<0.05 different from AT-403 alone. §p<0.05, different from AT-403 + SKF-38393. Three-way ANOVA followed by the Bonferroni post hoc test.

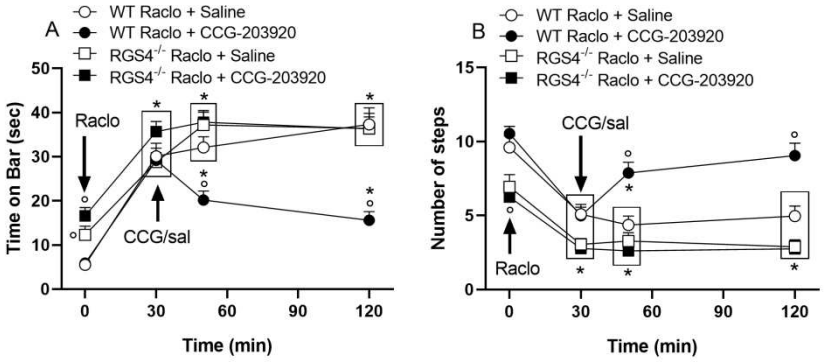

Figure 4. CCG-203920 reversed raclopride-induced-akinesia in wild-type (WT) but not in RGS4$^{-/-}$ mice. Immobility time in the bar test (in s; A) and number of steps in the drag test (B) were monitored before (baseline, time 0) and after the administration of 1 mg kg^{-1} of the D2 receptor antagonist raclopride (i.p.), followed 30 min later by the experimental RGS4 chemical probe CCG-203920 10 mg kg^{-1} or saline (i.p.). Arrows indicate the time of drug administration. Data are mean ± SEM of n=10 determinations per group, obtained from 10 WT and 10 RGS4$^{-/-}$ mice treated under a crossover design. *p< 0.05, different from baseline; °p<0.05, different from raclopride in WT mice (two-way RM ANOVA followed by the Tukey post hoc test).

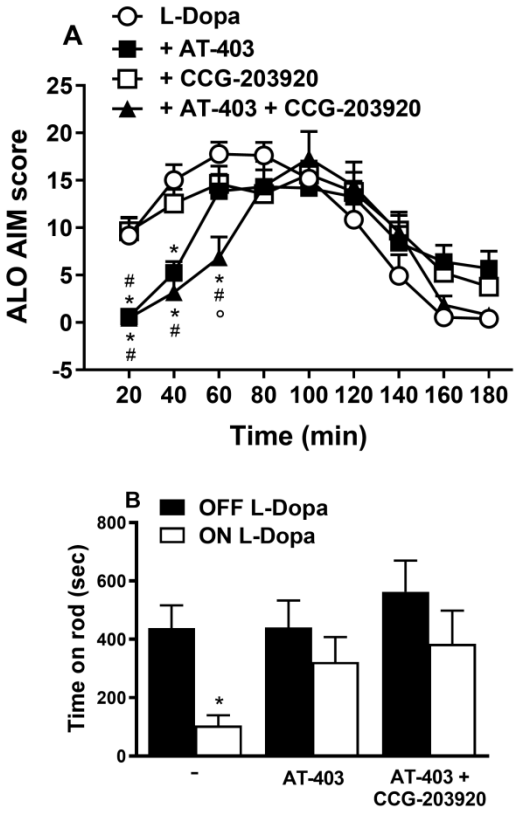

Figure 5. CCG-203920 extended the antidyskinetic effect of AT-403 without worsening motor performance on the rotarod. (A) ALO AIMs were scored in 6-OHDA hemilesioned dyskinetic rats following challenge with L-Dopa (6 mg kg^{-1} plus benserazide 15 mg kg^{-1}, s.c.) combined with vehicle, the NOP receptor agonist AT-403 (0.03 mg kg^{-1}, s.c.) or the experimental RGS4 chemical probe CCG-203920 (10 mg kg^{-1}, i.p) (A). Values are mean ± SEM of 13 rats per group. *p<0.05, **p<0.01, different from L-Dopa; ## p<0.01, different from L-Dopa + CCG-203920; °p<0.05, different from L-Dopa + AT-403. Two-way repeated measure ANOVA followed by the Tukey post hoc test. (B) Rotarod performance was evaluated as time on rod in seconds, before (OFF) and 60 min after (ON) L-Dopa (6 mg kg^{-1} plus benserazide 15 mg kg^{-1}, s.c.) combined with vehicle, AT-403 (0.03 mg kg^{-1}, s.c.) or CCG-203920 (10 mg kg^{-1}, i.p.). Values are mean ± SEM of 11 rats per group. *p<0.05, different from OFF L-Dopa (Student t-test, two tailed for unpaired data).

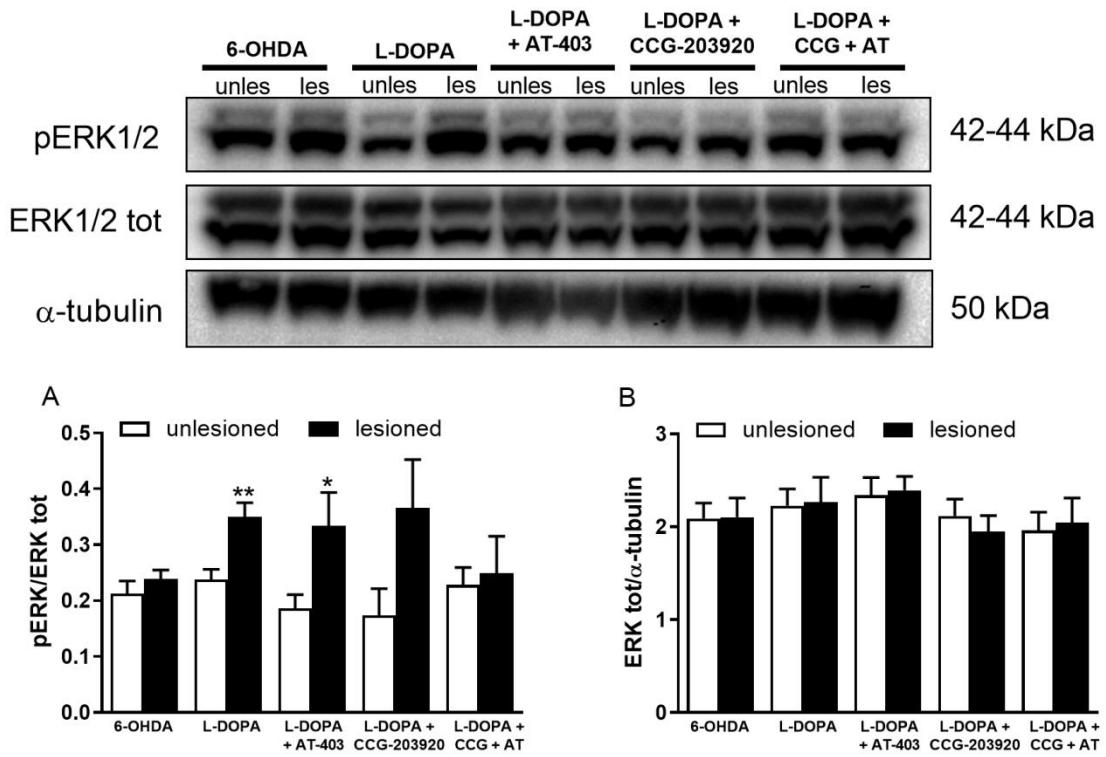

Figure 6. AT-403 in combination with CCG-203920 inhibited L-Dopa-induced ERK phosphorylation in the striatum of dyskinetic rats. Western blot representative images (upper panel) and quantification (lower panel) of pERK (A) and total ERK (B) in the lesioned and unlesioned striatum of 6-OHDA hemilesioned L-Dopa-naïve or dyskinetic rats. Dyskinetic rats were treated with the NOP receptor agonist AT-403 (0.03 mg kg^{-1}, s.c.) or vehicle and, 10 min later, challenged with L-Dopa (6 mg kg^{-1}, i.p.). The experimental RGS4 chemical probe CCG-203920 (10 mg kg^{-1}, i.p.) or vehicle were administered 5 min before AT-403. Values are mean ± SEM of 6 rats per group. *p<0.05, different from unlesioned striatum (Student t-test, two-tailed for unpaired data).

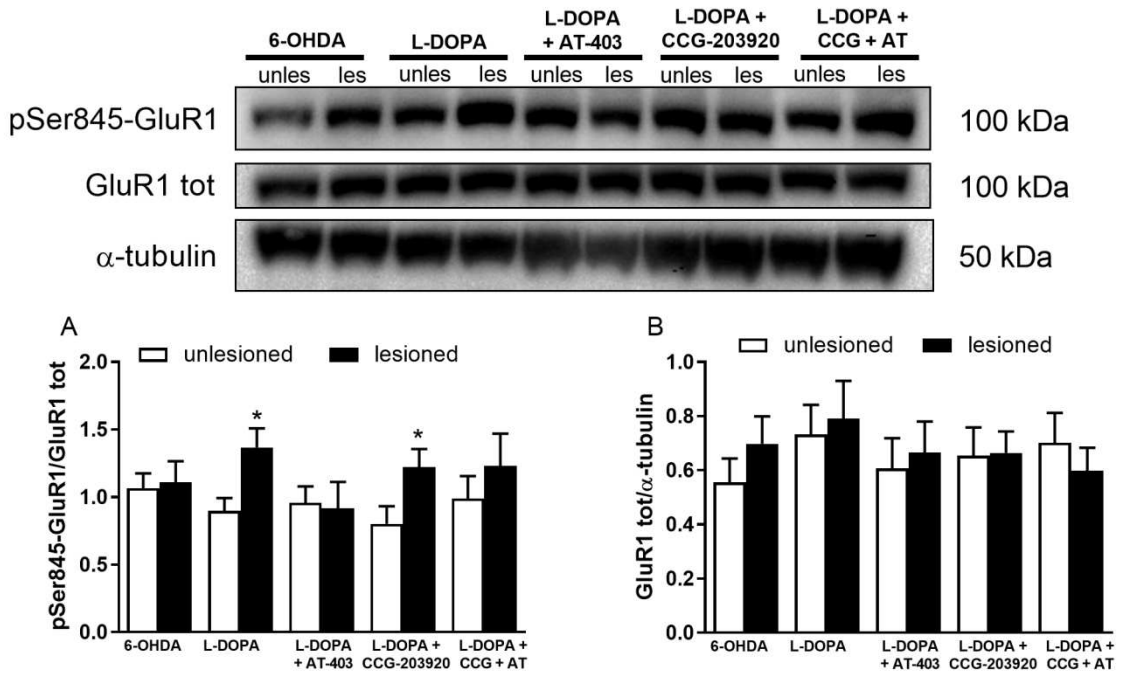

Figure 7. AT-403 inhibited the L-Dopa-stimulated pGluR1 phosphorylation in the striatum of dyskinetic rats. Western blot representative images (upper panel) and quantification (lower panel) of pGluR1 (A) and total GluR1 (B) in the striatum of 6-OHDA hemilesioned, L-Dopa-naïve or dyskinetic rats. Dyskinetic rats were treated with the NOP receptor agonist AT-403 (0.03 mg kg^{-1}, s.c.) or vehicle and, 10 min later, challenged with L-Dopa (6 mg kg^{-1}, i.p.). The experimental RGS4 chemical probe CCG-203920 (10 mg kg^{-1}, i.p.) or vehicle were administered 5 min before AT-403. Values are mean ± SEM of 6 rats per group. *$p<0.05$, different from unlesioned striatum (Student t-test, two-tailed for unpaired data).

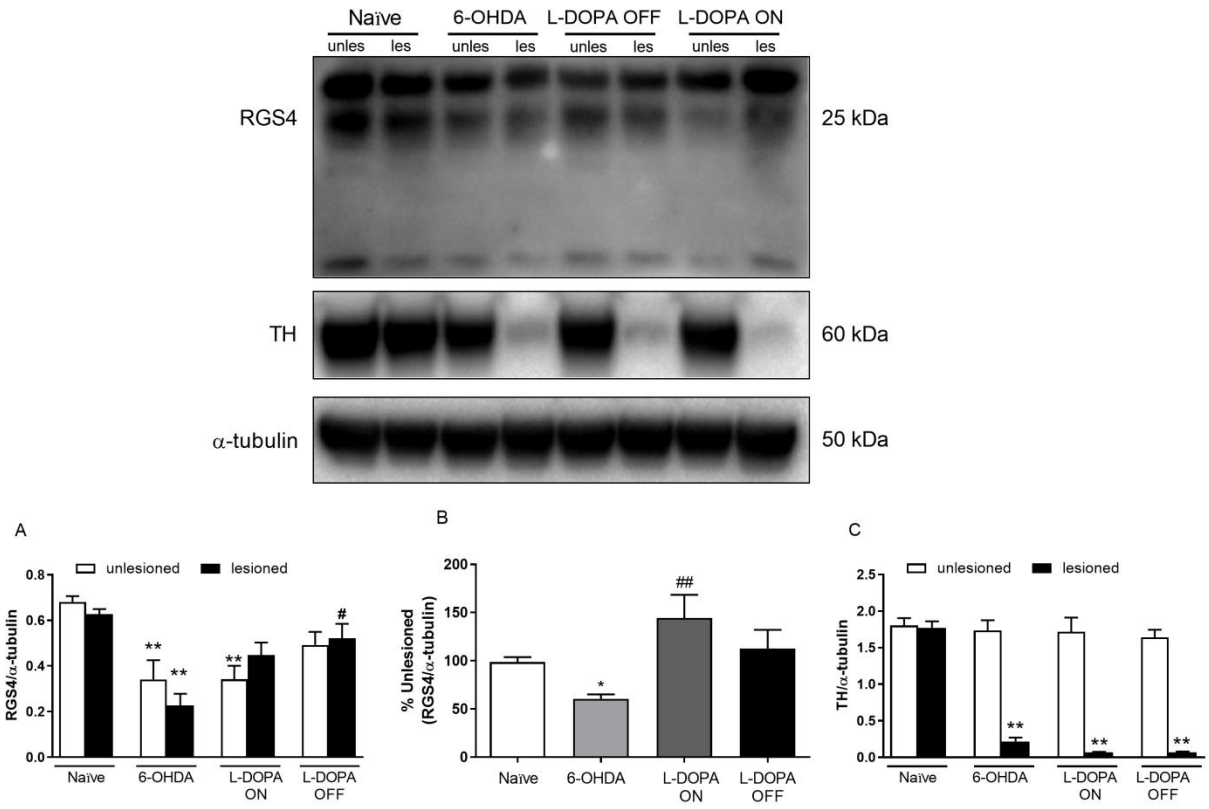

Figure 8. RGS4 levels were modulated by 6-OHDA and L-DOPA treatment. Western blot representative images (upper panel) and quantification (lower panel) of RGS4 in the striatum of naïve, 6-OHDA hemilesioned L-Dopa naive, or dyskinetic rats. In dyskinetic rats, RGS4 analysis was carried out both OFF and ON L-Dopa. RGS4 values were normalized to alpha-tubulin as housekeeper and expressed as absolute values (A) or percentage of RGS4 in the lesioned relative to unlesioned striatum (B). Tyrosine hydroxylase levels normalized to alpha-tubulin are also shown (C). Values are mean ± SEM of 7 rats per group (n=6 in the ON L-Dopa group due to animal loss. In panel B, one outlier was removed from the 6-OHDA group). *p<0.05, different from naïve (A-B) or unlesioned striatum (C); #p<0.05 different from 6-OHDA (B). One-way ANOVA followed by the Newman-Keuls test (A), Kruskal-Wallis test followed by the Dunn test (B). Student t-test, two-tailed for unpaired data (C).